ORIGINAL STUDY

NUMERICAL SIMULATION OF THE PROCESS OF COLD GAS-DYNAMIC SPRAYING OF COMPOSITE POWDER Al–Zn–TiO_2

Kaiyrzhan Berikkhan[1,2], Zarina Satbayeva[1], Ainur Zhassulan[1], Aibek Shynarbek[1], Kuanysh Ormanbekov[1]

[1] Engineering Center, Shakarim University, st. Fizkulturnaya 4B, Semey, Kazakhstan;
[2]Department of Technical Physics and Heat Power Engineering, Research School of Physical and Chemical Sciences, Shakarim University of Semey, Republic of Kazakhstan
*Corresponding author: k.berikkhan@shakarim.kz

Abstract. *This paper presents a numerical simulation of the cold gas-dynamic spraying process of Al-Zn-TiO_2 composite powder onto a steel substrate. Using computational fluid dynamics (CFD) in COMSOL Multiphysics, the characteristics of the gas flow in a de Laval nozzle and the particle dynamics are obtained for various spraying parameters. Optimal conditions are determined: gas pressure of approximately 0.6 MPa, temperature of ~600°C, nozzle-to-substrate distance of 15 mm, spray angle of 90°. At these conditions, particles reach supersonic velocities of approximately 500-600 m/s, sufficient for their deposition on steel. It is shown that increasing gas pressure and temperature facilitates particle acceleration and increases their impact energy, while excessively small or large spraying distances reduce the efficiency of the process. Simulation of the impact interaction of particles with the substrate revealed intense plastic deformation of the powders under optimal parameters, ensuring strong adhesion of the coating to the base. The results of the numerical experiment are consistent with the observed characteristics of dense and adhesion-strong coatings. It has been established that the proposed CFD model can be used as an effective tool for optimizing the parameters of cold gas-dynamic spraying of composite powders.*

Keywords:cold gas-dynamic spraying; numerical modeling; CFD; composite coating; aluminum-zinc-titanium dioxide; particle velocity; critical velocity; plastic deformation.

1. Introduction

Cold Gas Dynamic Spray (CGDS) is a solid-phase coating application method in which powder particles are accelerated to high velocities by a heated, compressed gas stream and deposited onto a substrate by high-speed impact without melting [1, 2]. Since the particles are not heated to the melting temperature, the coating is formed without oxidation or other thermal damage to the base material [3]. The result is dense, low-porosity coatings with predominantly compressive residual stresses [4]. CGDS allows coating heat-sensitive materials without overheating and preserving the original powder microstructure [5].

Currently, the CGDN method is successfully used to deposit various materials-pure metals, alloys, and metal-matrix composites [6, 7]. The particles bond to the substrate through their strong plastic deformation upon impact, which leads to the formation of a strong interfacial bond without melting [8]. It is known that certain impact conditions are necessary for successful particle deposition-in particular, the particle velocity must exceed a critical value that ensures adhesion of a given material to the substrate [9, 10]. For example, for aluminum on steel, the critical velocity is approximately 500 m/s [9, 10]. If the particle moves more slowly, it will not adhere to the surface, so reaching and exceeding the critical velocity is a key factor in the process.

The velocity and energy of the particles are affected by the process parameters of the CGDN: gas pressure and temperature, nozzle geometry, nozzle-to-substrate distance (nozzle overhang), particle size, and spray angle [11, 12]. Increasing the gas pressure and temperature increases the flow velocity and particle acceleration due to an increase in the pressure gradient and a decrease in the gas density [13, 14]. Reducing the nozzle overhang (spraying too close) can lead to under-acceleration of the particles and their flattening against the

Received 5 December 2025; revised 17 December 2025; accepted 5 January 2026.
Published online 20 March 2026

(https:doi.org/……)

substrate, while an excessively large overhang leads to dispersion and deceleration of the particles in the air [15, 16]. Each powder material has its own critical deposition velocity; for Al-Zn-TiO_2 composite particles, it is determined mainly by the properties of the aluminum matrix (about 500 m/s), since it is the ductile aluminum that ensures adhesion to the substrate. Zinc, being a softer metal, has a lower critical velocity. However, its presence promotes anodic protection and does not impair adhesion. Solid TiO_2 particles dispersed in aluminum increase coating hardness but have virtually no effect on adhesion once the matrix reaches the required velocity. Therefore, modeling requires taking into account the multicomponent nature of the powder, but critical deposition conditions are, as a first approximation, estimated for aluminum.

Experimental optimization of the CGDN process requires repeated parameter variations and coating quality analysis, which is time-consuming and resource-intensive. Therefore, numerical modeling plays an important role in predicting the behavior of the gas flow and particles under various spraying conditions [17, 18]. Computational fluid dynamics (CFD) and impact mechanics methods allow one to determine the velocity and temperature distribution in the jet, particle trajectories and velocities, their temperature, and the stresses upon collision with the substrate. Such models are used to estimate critical velocities and the boundaries of the "deposition window" - the ranges of parameters within which a high-quality coating is formed [19]. In this study, a comprehensive CFD modeling of the CGDN of Al-Zn-TiO_2 composite powder on steel was performed. The goal of the modeling is to determine the parameters at which maximum velocity and efficient particle deposition are achieved, and thereby substantiate the optimal process conditions.

2. Materials and methods

The numerical model was developed in COMSOL Multiphysics AB (v6.2) and includes a coupled analysis of gas flow, particle motion, and impact on the substrate. Deposition onto a flat steel substrate was considered using a 100 mm long de Laval nozzle (convergent-divergent) with a throat diameter of 2 mm and an outlet diameter of 6 mm. The calculations included the inner region of the nozzle and the outer section from the nozzle exit to the substrate surface (Fig. 1). The model is axisymmetric (3D with a degree of symmetry), which is justified by the axial nature of the flow.

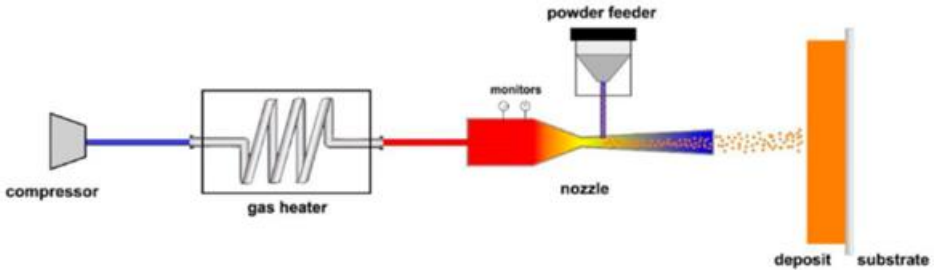

Fig. 1. Installation diagram and calculated setting of the gas turbine.

Turbulent compressible flow equations (RANS, k-ε model) were solved for air as the working gas. The total (stagnation) pressure P0 and temperature T_0 were specified at the nozzle inlet, and the atmospheric pressure of 0.1 MPa was specified at the nozzle outlet. The nozzle walls were assumed to be adiabatic and non-slip. Initial calculations were performed at P0 = 6×105 Pa and T0 = 600 °C (873 K), which corresponds to typical operating conditions.

When flowing through a convergent-divergent nozzle, the gas expands to supersonic speeds-in our case, the calculated exit flow reached ≈1200 m/s at P0 = 0.6 MPa and T0 = 600 °C. Due to adiabatic expansion, the gas temperature in the jet core decreased to approximately ~327 °C. The supersonic core region extended from the nozzle exit to the substrate, forming the so-called "patch" of the shock jet on the surface.

The composite powder particles were defined as a discrete Lagrangian phase (using the Particle Tracing module in COMSOL) in one-way coupling with the gas-that is, the effect of the particles on the flow was neglected due to their low concentration. For simplicity, all particles were assumed to be spherical (in reality, Al-Zn powder has an irregular shape, but for computational efficiency, an equivalent sphere was adopted). The particle diameter was assumed to be 20 μm as representative (fraction 20-50 μm); the material density was ~2700 kg/m³ (close to aluminum, given that the composition is 80% Al + 15% Zn + 5% TiO_2).

Particles were introduced into the flow at the nozzle throat with initial velocities equal to the local gas velocity (zero slip during introduction). The particles were subjected to drag forces (aerodynamic drag), taking

into account the Cunningham correction for small particles, as well as gravity, the effect of which is insignificant for a horizontal spray axis. Interparticle interactions were neglected (rarefied flow).

It was assumed that the particles would not melt or disintegrate during the process-which is justified, since the gas temperature, although high, has a short flight time, and aluminum begins to melt at 660°C; calculations show that the particle temperature does not reach the melting point.

The substrate was modeled as a stationary solid wall; upon particle contact with the substrate, the solution was transferred to the Solid Mechanics module to evaluate deformation. An elastoplastic impact model was used to evaluate the stress-strain state upon particle impact with the substrate: the particle material (primarily aluminum) was described by an elastoplastic model with a yield strength of ~100 MPa, and the substrate material (steel) was described by a yield strength of ~250 MPa. These values correspond to soft Al-Zn powder and St3 steel, respectively. Impact modeling allowed us to assess whether plastic deformations develop in the particle and substrate and whether they are sufficient to form an adhesion contact area.

To study the influence of spraying conditions, a series of calculations were performed with various parameters. The main variable values were: gas pressure P0 (0.4; 0.5; 0.6 MPa), temperature T0 (400; 500; 600 °C), and nozzle offset d (distance from the outlet section to the substrate: 5; 15; 25 mm). The spray angle remained perpendicular (90° to the surface) in all experiments. Each calculation was performed until a steady-state flow regime was established and the particles reached the substrate.

To ensure statistical reliability, the trajectories were modeled for a packet of 100 particles uniformly distributed across the flow cross-section at the inlet. A separate high-precision calculation was also performed for optimal parameters with a fine time step (0.1 μs) for a detailed impact analysis.

For computational stability and reproducibility, standard simplifications for cold spraying were adopted:

1. The sphericity of the particles (although real Al-Zn particles have an irregular shape and contain TiO_2 agglomerates) simplifies the calculation of aerodynamic drag and momentum transfer.
2. The 20 μm monofraction is used as a representative size (actually ~20-50 μm according to specification and SEM); the size distribution was not explicitly modeled.
3. Absence of interparticle collisions and agglomeration in flight; one-way connectivity (particles do not affect the gas).
4. Solid state of particles throughout the entire path (without melting/destruction) and constant properties of materials.
5. The initial particle velocity is equal to the local gas velocity at injection. These assumptions focus the analysis on the key physics of acceleration and impact and make the model computationally tractable.

3. Results and discussion

Computational fluid dynamics predicted that at a pressure of 0.6 MPa and 873 K, the nozzle forms a supersonic jet with a gas discharge velocity of up to ~1200 m/s (Fig. 2a). Under these conditions, Al-Zn-TiO2 particles accelerate to terminal impact velocities of approximately 600-700 m/s at a distance of 15 mm (Fig. 2c). Shorter distances (e.g., 10 mm) lead to underexpansion of the flow and excessive impact forces, while larger distances (>25 mm) allow the particles to decelerate, reducing the impact velocity below the critical threshold for bond formation.

The impact model showed that upon impact, the particles experienced severe plastic deformation and flattened into disc-shaped splats. The von Mises stress within the particle peaked at approximately 300 MPa, confirming localized plastic flow (Fig. 2b). To put an impact stress of 300 MPa in context, this level is an order of magnitude higher than the yield strength of pure aluminum (on the order of only tens of MPa) and comparable to or even higher than the yield strength of mild steel (approximately 250 MPa). This high von Mises stress confirms that the particle moves well beyond its elastic limit, experiencing severe plastic flow, while the substrate surface is also locally fluid. These extreme stress and strain rate conditions favor the formation of adiabatic shear instability (a localized shear band with thermal softening) at the impact boundary rather than bulk melting of the material [20]. In other words, bonding remains a solid-state process dominated by intense plastic deformation and interfacial heating, with no evidence of localized melting or uncontrolled shear failure. Thus, the observed deformation and interfacial loading state are consistent with metallurgical solid-state bonding via plastic deformation, rather than indicating any melting or adiabatic shear instability that compromises the integrity of the deposit. In the substrate region immediately beneath the particle, a stress field approaching the yield strength was observed, resulting in shallow indentation and minor plastic

deformation, but without significant damage to the substrate. The high strain rate and localized heating facilitated the formation of an adiabatic shear layer, facilitating metallurgical bonding.

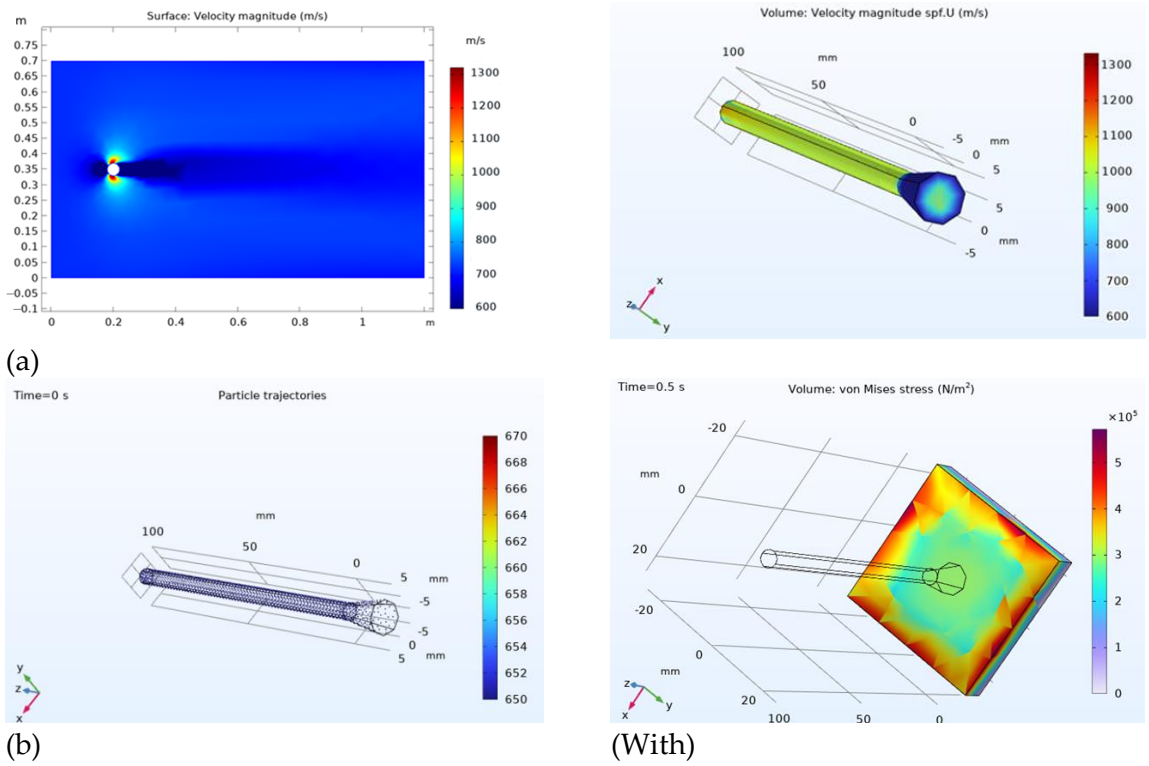

Fig. 2. (a) Surface plot and three-dimensional slice of the velocity magnitude in the midplane; (b) particle trajectories in the nozzle plume; (c) von Mises stress distribution in the substrate at the moment of particle impact.

The simulation results showed that the adhesion efficiency increased significantly with increasing gas pressure and temperature, reaching a stable regime at temperatures above ~0.6 MPa and 600 °C. Based on these data, the cold spraying process was carried out at a temperature of 600 °C, 0.6 MPa, and a distance from the surface of about 15 mm with a moderate powder feed rate (~0.5 g/s), since these parameters ensured sufficient particle velocity and deformation for metallurgical bonding. The resulting coatings had a dense lamellar structure without signs of delamination, which is consistent with the results of previous studies emphasizing the crucial role of impact conditions in ensuring adhesion [21, 22].

Numerical simulations in COMSOL Multiphysics provided a detailed understanding of the sputtering process. The gas jet reached supersonic speeds, creating a high-velocity core in which particles accelerated to 500-600 m/s under optimal conditions (0.6 MPa, 600°C, 15 mm standoff, 90° spray angle) (Fig. 2a). Impact simulations showed that these velocities generated sufficient plastic deformation and interfacial stress for effective adhesion. Curved surface simulations showed that particle impact velocities decreased slightly at the edges due to deflection, explaining the minor thickness variations. Numerical predictions matched experimental trends for deposition efficiency, roughness, and coating quality, confirming the model's reliability as a tool for process optimization.

Optimal deposition parameters were determined based on a comprehensive analysis of gas-dynamic modeling and experimental observations. Coatings deposited at a gas pressure of 0.6 MPa, a gas temperature of 600°C, and a distance from the electrode of 15 mm demonstrated the most favorable microstructural characteristics: dense particle packing, a uniform layered structure, and the absence of delamination.

To confirm the choice of optimal sputtering conditions, a series of computational fluid dynamics calculations were performed at a constant gas temperature of 800 K and a fixed nozzle-to-substrate distance of 0.01 m, while the working gas pressure varied from 4 × 105 Pa to 6 × 105 Pa. The gas and particle flow velocity fields were visualized for each condition (Fig. 3a-c). The simulation results clearly show that increasing the pressure leads to a significant increase in the particle velocity at the nozzle outlet.

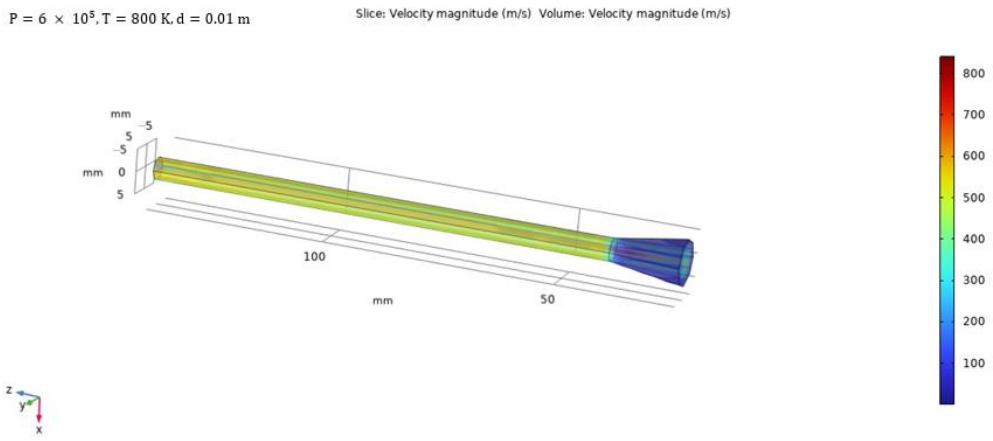

(a)

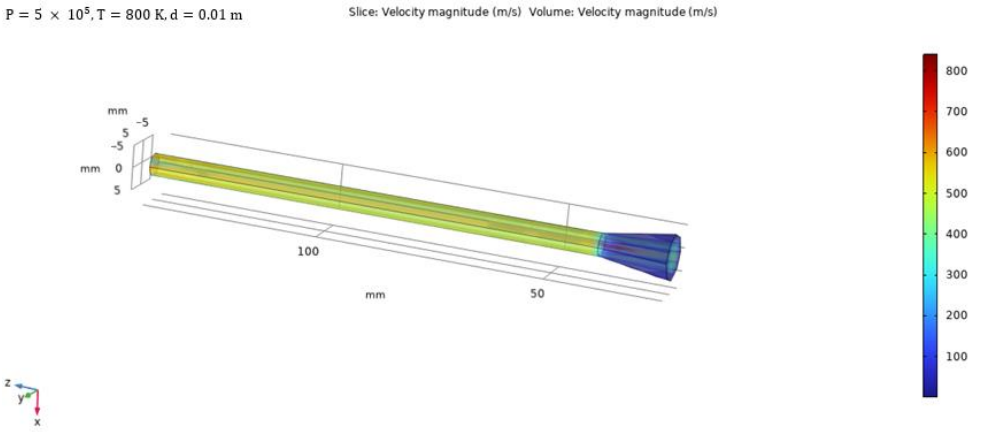

(b)

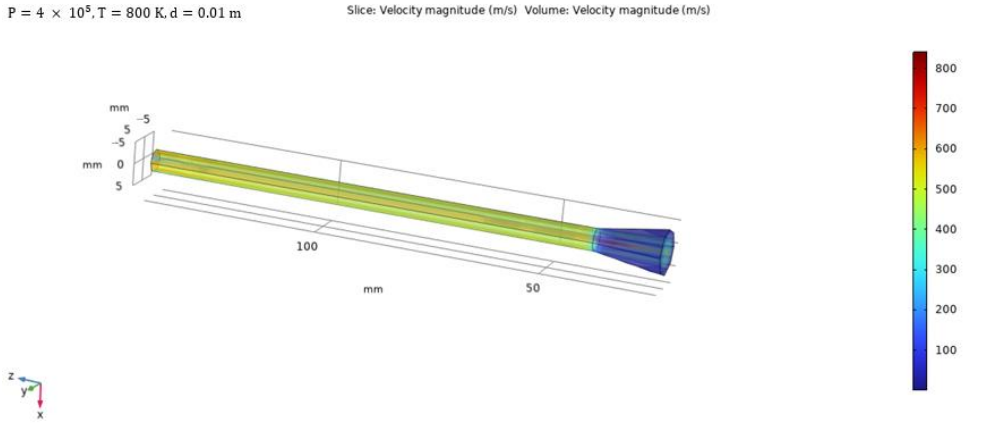

(With)

Fig. 3. (a) Velocity distribution at P = 6 × 105 Pa, T = 800 K, d = 0.01 m;(b) Velocity distribution at P = 5 × 105 Pa, T = 800 K, d = 0.01 m;(c) Velocity distribution at P = 4 × 105 Pa, T = 800 K, d = 0.01 m.

At a pressure of 4 × 105 Pa, the maximum particle velocity was approximately 620 m/s. At a pressure of 5 × 105 Pa, it increased to approximately 710 m/s. At a pressure of 6 × 105 Pa, the particle velocity exceeded 820 m/s. This indicates that higher chamber pressure leads to greater particle acceleration due to increased pressure gradients along the nozzle. Since particle velocity directly affects the deposition behavior (e.g., the degree of particle deformation upon impact and adhesion), the conditions P = 6 × 105 Pa and T = 800 K are considered optimal for producing high-quality coatings.

Fig. 4a and 4b show the temporal evolution of the gas temperature field inside the nozzle from t = 0 s to t = 0.05 s, simulated with a time step of 0.001 s. At the initial instant (t = 0 s), the temperature remains relatively

uniform along the entire length of the nozzle and is ~800 K, indicating stable initial thermal conditions (Fig. 4a). As the simulation progresses, by t = 0.05 s (Fig. 4b), a pronounced temperature gradient arises, with higher temperatures concentrated near the nozzle walls and inlet, and cooler regions located downstream. This behavior indicates adiabatic expansion and energy dissipation of the working gas along the nozzle. Localized heating zones indicate the development of a boundary layer, which affects both the gas velocity and the thermal energy transfer by particles.

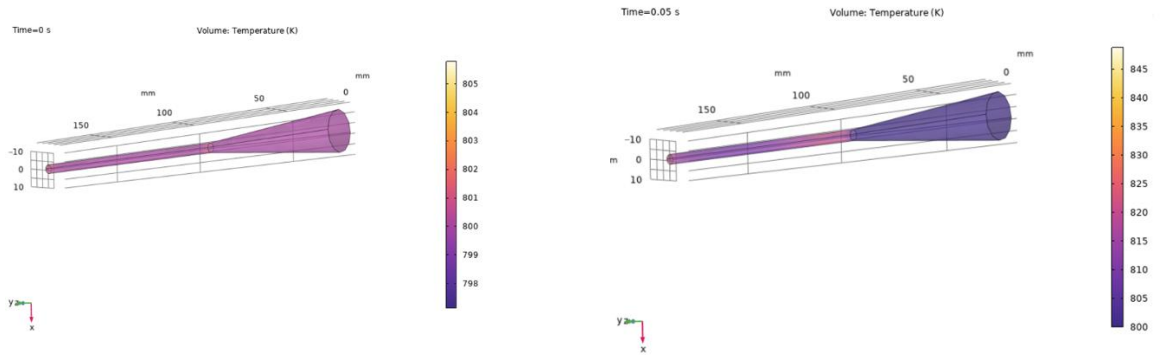

(a) (b)

Fig. 4. Temperature distribution in the spray jet at times (a) 0 s and (b) 0.05 s.

Fig. 5 shows the evolution of particle trajectories over the simulation interval from 0 to 0.05 s. The data was obtained with high temporal resolution (0.001 s step). The simulation reflects the behavior of particles under the influence of a supersonic gas jet during cold spraying.

At time = 0 s, the particles are densely grouped near the nozzle entrance, indicating their injection into the flow with an initially uniform spatial distribution (Fig. 5a). By time = 0.05 s, the particles have advanced significantly along the nozzle axis, forming a focused, high-speed flow (Fig. 5b). Convergence toward the centerline indicates effective particle acceleration and aerodynamic focusing, due to the nozzle geometry and gas flow dynamics.

This trajectory evolution is crucial, as it directly correlates with particle impact velocity and deposition efficiency. The highest particle density reaching the substrate is observed in the stagnation region near the nozzle exit, ensuring efficient coating formation under the simulated pressure and temperature conditions.

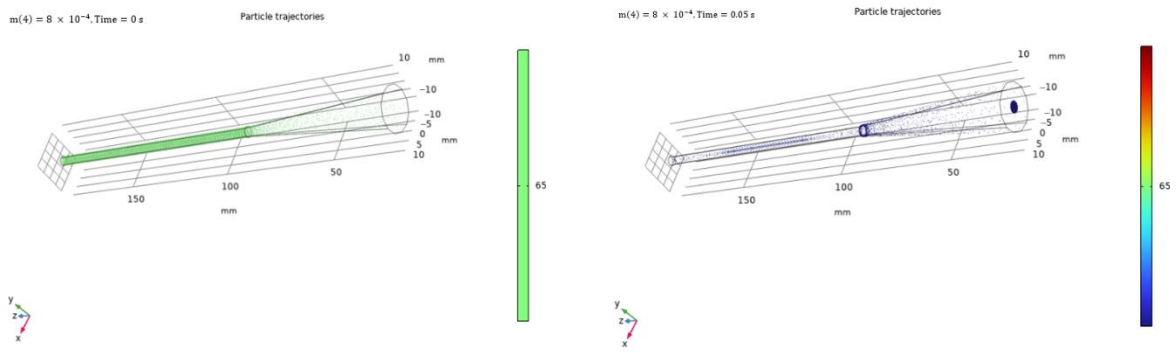

(a) (b)

Fig. 5. (a) Particle trajectories at t = 0 s; (b) Particle trajectories at t = 0.05 s.

Computational fluid dynamics (CFD) and thermal modeling calculations confirmed that increasing the gas pressure from 4 × 105 Pa to 6 × 105 Pa (at a gas temperature of 800 K) leads to a significant increase in particle exit velocity, exceeding 650 m/s at maximum pressure. This indicates increased deposition potential at elevated driving forces. Modeling also identified a distance of ~15 mm as favorable, where particles maintain high velocity and focus on the substrate surface, promoting efficient deposition and uniform coating growth. Thermal modeling showed that the gas temperature on the substrate after expansion remained around 500 K, significantly below the melting point of the materials, preventing thermal degradation.

The particle flight velocities predicted by the model were compared with experimental data to assess the model's validity. CFD simulations showed that under optimal spraying conditions (gas pressure of ~0.6 MPa, gas temperature of ~600°C, and a 15 mm offset), the particles would reach impact velocities of approximately 500-600 m/s. This predicted velocity range exceeds the typical critical velocity (~500 m/s) required for aluminum particles to adhere to a steel substrate. As predicted, coatings were successfully deposited at 0.6 MPa and 600°C with strong adhesion, indicating that the particles indeed achieved velocities high enough to exceed the adhesion threshold. In contrast, at lower stagnation pressures (0.4 MPa) or gas temperatures (400°C), the model predicted a significant reduction in particle velocity, and experiments under these conditions resulted in either very poor adhesion or no coating deposition, indicating that the particles did not reach critical velocity in these cases. Although direct measurement of particle velocity was not available in our setup, these qualitative results (the presence or absence of an effective coating) provide indirect confirmation of the modeling results. Furthermore, the model correctly captured the effect of standoff distance on particle velocity and deposition: it predicted an optimal standoff window of approximately 10-20 mm (with ~15 mm being ideal) and showed that extreme standoff distances would be detrimental (particles would experience excessive drag at large distances or incomplete acceleration at very short distances). This behavior was confirmed experimentally: for example, at a distance of 5 mm, the high-velocity gas jet caused particle splashing and substrate abrasion instead of effective deposition, while at a distance of 25 mm, the particles slowed down and led to insignificant coating buildup. Such close agreement between simulated particle velocities and experimental results convincingly confirms the accuracy of the COMSOL model. In particular, the model's ability to predict successful and unsuccessful deposition conditions (via velocity thresholds and trends) confirms its credibility as a reliable predictive tool for optimization and parameter selection in the cold gas dynamic spraying process.

4. Conclusion

Numerical modeling of the CGD process for Al-Zn-TiO_2 powder allowed us to identify the optimal parameters for efficient coating deposition. It was found that at a gas pressure of approximately 0.6 MPa, a temperature of approximately 600°C, a nozzle-to-substrate distance of approximately 15 mm, and a perpendicular spray angle (~90°), particles accelerate to supersonic velocities (~500-600 m/s), exceeding the critical deposition velocity of aluminum on steel (approximately 500 m/s). Achieving this velocity ensures intense plastic deformation of the particles upon impact and strong adhesion of the coating to the substrate without melting the material. It has been shown that increasing the pressure (up to ~0.6-0.7 MPa) and gas temperature (up to ~600-800 °C) leads to an increase in the particle velocity at the nozzle outlet and, consequently, to an increase in their impact energy, which contributes to an increase in the efficiency of forming a dense and adhesively strong coating. Conversely, deviations from the optimal spraying distance negatively affect the process: too small an extension (e.g., 5 mm) leads to insufficient particle acceleration and the effects of scattering and erosion of the substrate by the high-speed jet, while too large an extension (e.g., 25 mm) causes the particles to slow down in the air and reduce their ability to attach to the surface. Thus, the existence of a "spraying window" is confirmed – a range of distances of approximately 10-20 mm (for the given conditions) within which maximum deposition efficiency is achieved (with an optimum of approximately 15 mm), while going beyond this range sharply reduces the coating quality.

A key result is the identification of the particle adhesion mechanism: upon impact at supersonic speed, stresses and strains develop in the particle material that significantly exceed the yield strength (estimated equivalent stresses of ~300 MPa for aluminum), indicating severe plastic deformation without melting. Simulation confirmed the formation of a local adiabatic shear band upon impact, which facilitates the destruction of the oxide film and metallurgical adhesion at the interface without melting. Thus, the numerical model reliably describes the physics of the cold spray process and can serve as an effective tool for predicting and optimizing its parameters. The obtained results are consistent with literature data and experimental observations, and the developed model has practical significance for managing the quality of cold sprayed coatings.

Funding

This work does not receive any funding.

Conflict of interest

The authors declare no conflict of interest.

References

1 Klinkov SV, Kosarev VF, Rein M. (2005) Significance of particle impact phenomena in cold spray deposition. *Aerospace Science and Technology*. Vol.9, No.8. P.582–591

2 Alkhimov AP, Kosarev VF, Klinkov SV (2001) The features of cold spray nozzle design. *Journal of Thermal Spray Technology*. Vol.10, No.2. P.375–381

3 Papyrin A., Kosarev V., Klinkov S., Alkhimov A., Fomin V. (2006) Cold Spray Technology. *Amsterdam: Elsevier*, 336

4 Champagne VK (Ed.) The Cold Spray Materials Deposition Process: Fundamentals and Applications. *Cambridge: Woodhead Publishing*, (2007). 360

5 Villafuerte J. (Ed.) Modern Cold Spray: Materials, Process, and Applications. *Berlin: Springer*, (2015). 345

6 Hassani-Gangaraj S.M., Moridi A., Guagliano M. (2015) Critical review of corrosion protection by cold spray coatings. *Surface Engineering*. Vol.31, No.12. 803–815

7 Assadi H., Kreye H., Gärtner F., Klassen T. Cold spraying - A materials perspective. Acta materialia. (2016). Vol.116. 382–407

8 Assadi H., Gärtner F., Stoltenhoff T., Kreye H. Bonding mechanism in cold gas spraying. Acta materialia. (2003). Vol.51, No.15. 4379-4394

9 Moridi A., Hassani-Gangaraj S.M., Guagliano M., Dao M. Cold spray coating: review of material systems and future perspectives. *Surface Engineering*. (2014). Vol.30, No.6. P.369–395

10 Yin S., Cavaliere P., Aldwell B., Jenkins R., Liao H., Li W., Lupoi R. Cold spray additive manufacturing and repair: fundamentals and applications. *Additive Manufacturing*. (2018). Vol.19. 628-650

11 Irissou É., Legoux J.-G., Ryabinin A.N., Jodoin B., Moreau C. Review on cold spray process and technology: Part I - Intellectual property. *Journal of Thermal Spray Technology*. (2008). Vol.17, No.4. 495-516

12 Pattison J., Celotto S., Morgan R., Bray M., O'Neill W. Cold gas dynamic manufacturing: a non-thermal approach to freeform fabrication. *International Journal of Machine Tools and Manufacture*. (2007). Vol.47, No.3-4. 627-634

13 Dykhuizen RC, Smith MF Gas dynamic principles of cold spray. *Journal of Thermal Spray Technology*. 1998. Vol.7, No.2. 205-212

14 Gilmore DL, Dykhuizen RC, Neiser RA, Smith MF, Roemer TJ Particle velocity and deposition efficiency in the cold spray process. *Journal of Thermal Spray Technology*. (1999). Vol.8, No.4. 576–582

15 Stoltenhoff T., Kreye H., Richter H.J. An analysis of the cold spray process and its coatings. *Journal of Thermal Spray Technology*. (2002). Vol.11, No.4. 542-550

16 Schmidt T., Gärtner F., Assadi H., Kreye H. Development of a generalized parameter window for cold spray deposition. *Acta materialia*. (2006). Vol.54, No.3. 729-742

17 Grujicic M., Zhao CL, DeRosset WS, Helfritch DJ Adiabatic shear instability-based mechanism for particle bonding in the cold-gas dynamic-spray process. *Applied Surface Science*. (2003). Vol.219, No.3-4. 211-227

18 Meng XM, Zhang JB, Liang YL, Han W., Zhao J. Effect of gas temperature on deposition behavior in cold spray. *Surface and Coatings Technology*. (2008). Vol.202, No.18. 4470-4477

19 Yu T., Chen M., Wu Z. Experimental and numerical study of deposition mechanisms for cold spray additive manufacturing process. *Chinese Journal of Aeronautics*. (2022). Vol. 35, No. 2. 276-290

20 Li W.-Y., Zhang C., Guo XP, Zhang G., Liao HL, Coddet C. Deposition characteristics of Al-12Si alloy coating fabricated by cold spraying with relatively large powder particles. *Applied Surface Science*. (2007). Vol. 253, No. 17. 7124-7130

21 Wang, N.; Liu, C.; Wang, Y.; Chen, H.; Chu, X.; Gao, J Effect of process parameters on properties of cold-sprayed Zn-Al composite coatings. *Materials* (2022), 15, 7007

22 Wang, K.; Wang, S.; Xiong, T.; Wen, D.; Wang, G.; Liu, W.; Du, H. Protective performance of ZnAlMgTiO_2 coating prepared by cold spraying on marine steel equipment. *Coatings* (2019), 9, 339

AUTHORS' INFORMATION

Berikkhan Kaiyrzhan - PhD student in Technical Physics, Engineering Center, Shakarim University, Semey, Kazakhstan; ORCID: 0009-0009-2788-062X; (e-mail: k.berikkhan@shakarim.kz)

Satbayeva Zarina - Professor - researcher at the Department of Technical Physics and Thermal Engineering, Shakarim University, Semey, Kazakhstan; ORCID: 0000-0001-7161-2686; (e-mail: satbaeva.z@mail.ru)

Zhassulan Ainur - PhD student in Technical Physics, Senior Researcher, Engineering Center, Shakarim University, Semey, Kazakhstan; ORCID: 0000-0001-5166-4761; (e-mail: a.zhassulan@shakarim.kz)

Shynarbek Aibek - PhD student in Technological Machines and Equipment, Engineering Center, Shakarim University, Semey, Kazakhstan; ORCID: 0009-0001-5887-0135; (e-mail: a.shynarbek@shakarim.kz)
Ormanbekov Kuanysh - PhD student in Technological Machines and Equipment,Engineering center,University name Shakarima,Semey,Kazakhstan; ORCID: 0000-0001-6099-2812; (e-mail: k.ormanbekov@shakarim.kz)